Avoiding fatal damage to the top electrodes when forming unipolar resistance switching in nano-thick material systems

2012 J. Phys. D: Appl. Phys. 45 255101

(http://iopscience.iop.org/0022-3727/45/25/255101)

IOP PUBLISHING JOURNAL OF PHYSICS D: APPLIED PHYSICS

J. Phys. D: Appl. Phys. **45** (2012) 255101 (6pp) doi:10.1088/0022-3727/45/25/255101

Avoiding fatal damage to the top electrodes when forming unipolar resistance switching in nano-thick material systems

S B Lee[1], D-H Kwon[2], K Kim[3], H K Yoo[1], S Sinn[1], M Kim[2], B Kahng[3] and B S Kang[4]

[1] ReCFI, Department of Physics and Astronomy, Seoul National University, Seoul 151-747, Korea
[2] Department of Materials Science and Engineering, Seoul National University, Seoul 151-744, Korea
[3] Department of Physics and Astronomy, Seoul National University, Seoul 151-747, Korea
[4] Department of Applied Physics, Hanyang University, Ansan, Gyeonggi-do 426-791, Korea

E-mail: bosookang@hanyang.ac.kr

Received 5 March 2012, in final form 24 April 2012
Published 7 June 2012
Online at stacks.iop.org/JPhysD/45/255101

Abstract
When forming unipolar resistance switching in material systems, fatal damage often occurs to the top electrodes of Pt/$SrTiO_x$/Pt, Pt/TiO_y/Pt and Pt/NiO_z/Pt cells. To develop a means of overcoming this problem, we systematically investigated the forming process by applying triangular- and pulse-waveform voltage signals to the cells. By investigating the dependence on sweep rate of the triangular-waveform voltage signals and amplitude of the pulse-waveform voltage signals, we discovered that the forming process occurred by two different mechanisms, irrespective of the material: either a thermally assisted dielectric breakdown or a purely electrical dielectric breakdown. During the former process, the top electrodes remained clean, even though oxygen bubbles formed on them. We observed that the top electrodes were blown off only for the latter (electrical) breakdown as a result of the formation of many conducting channels. We were able to overcome the fatal damage to the top electrodes by modifying the forming process into the thermally assisted dielectric breakdown.

(Some figures may appear in colour only in the online journal)

1. Introduction

Unipolar resistance-switching (URS) phenomena refer to the reversible resistance changes between stable resistance states driven by the application of electric fields [1–3]. From the early 1960s, these intriguing phenomena have been reported in numerous material systems, including oxides, sulfides, semiconductors and organics [4]. At the beginning of the 21st century, full-scale research was revitalized due to both fundamental scientific interest and potential technological applications [1–3, 5–9]. Among the many possible applications, next-generation nonvolatile memory, also known as resistance random-access memory (RRAM), is the one that has attracted the most attention [1–3, 5–9]. RRAM has been reported to show excellent device performance [1–3]. Many researchers have reported possible methods of increasing the integration density using a new concept, a three-dimensional stack structure without transistors [5, 6]. However, irrespective of these discovered and proposed merits and methods, there is still a considerable list of problems to be solved before RRAM can be practically realized.

One important issue is that the forming process for URS frequently causes physical deformation of the device electrodes [9]. As will be described below, the forming process is the first step in generating conducting channels inside the thin film. This fatal electrode damage currently precludes the adoption of URS in computing circuits. The lack of understanding of the physical mechanism of the forming process has left us with apparently insurmountable difficulties in developing a solution. Therefore, in this work, we have tried

to understand why fatal damage occurs to the top electrode during the forming process by systematically investigating the physical mechanisms in Pt/$SrTiO_x$/Pt, Pt/TiO_y/Pt and Pt/NiO_z/Pt cells.

2. Experimental methods

We fabricated $SrTiO_x$, TiO_y and NiO_z thin films on Pt-coated Si substrates using a pulsed laser deposition technique. The appropriate deposition conditions varied for the three films: the $SrTiO_x$ thin film was deposited at a substrate temperature of 600 °C and an oxygen pressure of 50 mTorr, the TiO_y film at 600 °C and 50 mTorr and the NiO_z film at room temperature and 5 mTorr. We used x-ray diffraction techniques to check that the $SrTiO_x$, TiO_y and NiO_z thin films were all polycrystalline, and transmission electron microscopy (TEM) and scanning electron microscopy to confirm that their thicknesses were approximately 60 nm, 150 nm and 150 nm, respectively. To measure the electrical properties of the devices at room temperature, we deposited $50 \times 50\ \mu m^2$-wide top Pt electrodes using a conventional photolithography technique. The cell forming process was then investigated by applying either a triangular- or a pulse-waveform-triggered voltage signal to the electrodes using a Yokogawa FG300 synthesized function generator. The resulting currents were measured using a Yokogawa DL1740 digital oscilloscope.

3. Results and discussion

3.1. Fatal damage of the top electrodes after the forming process

To obtain URS, a pre-requisite forming process is required in which a high voltage is applied to the cells. Figure 1(*a*) shows the current–voltage (I–V) curves of the URS in Pt/$SrTiO_x$/Pt cells. When we applied a positive voltage to the pristine state, the cell experienced an abrupt current increase at 6–8 V. For this irreversible forming process, we used a compliance current, I_{comp}, to protect the cell from permanent damage. By increasing I_{comp} up to 30 mA during the forming process, our Pt/$SrTiO_x$/Pt cells showed URS I–V curves. The URS required either positive or negative voltage to attain reversible changes between low- and high-resistance states. Our Pt/TiO_y/Pt and Pt/NiO_z/Pt cells also produced I–V curves for URS.

Unfortunately, under typical I–V measurement conditions, most of the top Pt electrodes were fatally damaged in the URS forming process. Figure 1(*b*) shows a topological image obtained using atomic force microscopy of the top Pt electrode of the Pt/$SrTiO_x$/Pt cell after the URS forming process. During this forming process, we swept the voltage up to 9 V for a duration of 10^{-3} s. After the forming process, the top Pt electrode was blown off, and a 20 μm-diameter hole was observed. In the line profile of the hole, indicated by the blue dotted line in figures 1(*b*) and (*c*), the depth of the blown-off area was similar to the thickness (≈60 nm) of the Pt electrode. This means that the electrode material was thoroughly delaminated and the bare surface of the oxide layer exposed. This

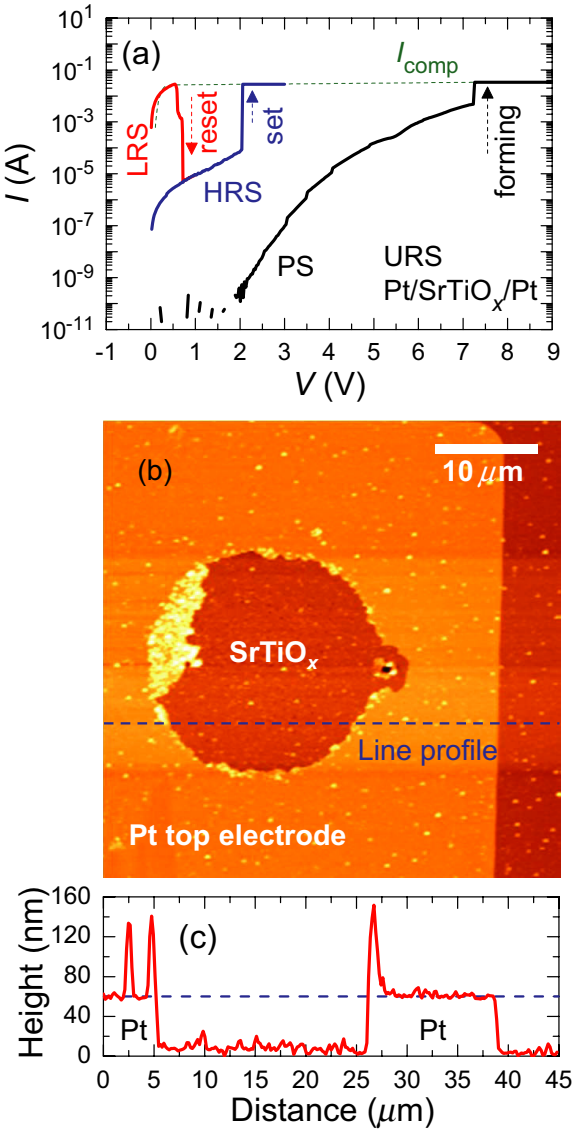

Figure 1. (*a*) I–V curves of URS in Pt/$SrTiO_x$/Pt cells. (*b*) Fatal damage in the top Pt electrode after the forming process. (*c*) A line profile of the blown-off area of the top Pt electrode.

fatal damage to the top electrodes is the major issue preventing RRAM realization [9, 10]. To understand why this fatal damage occurs, we investigated the physical mechanism of the URS forming process.

3.2. Physical mechanism of the forming process

We investigated the dependence of the sweep rate, $\nu \equiv V_t/t_t$, on the forming voltage V_F by applying a triangular-waveform voltage signal, designated by the subscript t. The amplitude of the signal, V_t, was fixed at 20 V and the duration of the voltage signal, t_t, was varied as indicated in figure 2(*a*). We measured the resulting current $I(t)$ as the triangular-waveform voltage signal, $V(t)$, was swept linearly with time, as shown in figures 2(*a*) and (*b*). When $V(t)$ reached the level V_F (figure 2(*a*)), $I(t)$ increased suddenly (figure 2(*b*)). This sudden increase in $I(t)$ indicates that percolating conductive channels were generated inside the

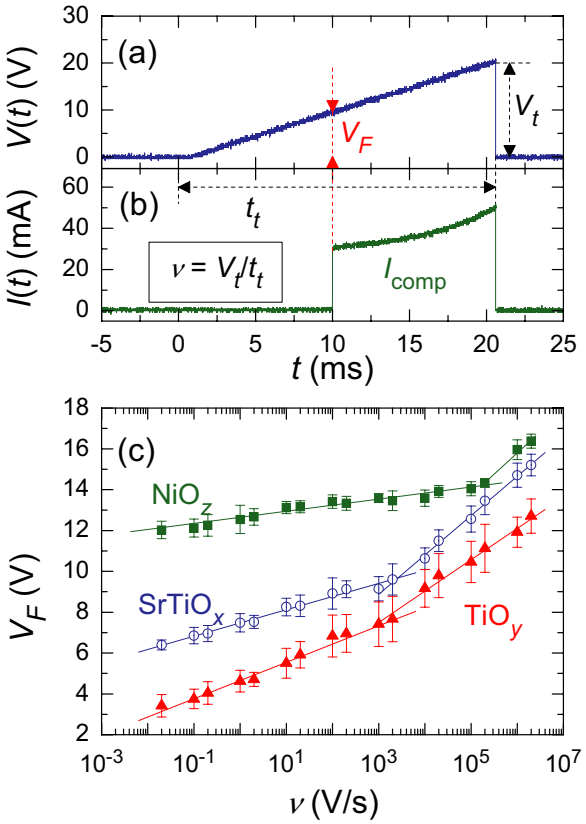

Figure 2. (*a*) Linear sweeping of a triangular-waveform voltage signal $V(t)$ with time t and (*b*) resulting current $I(t)$. (*c*) Sweep rate ν-dependence of the forming voltages V_F for Pt/SrTiO$_x$/Pt [12], Pt/TiO$_y$/Pt and Pt/NiO$_z$/Pt cells.

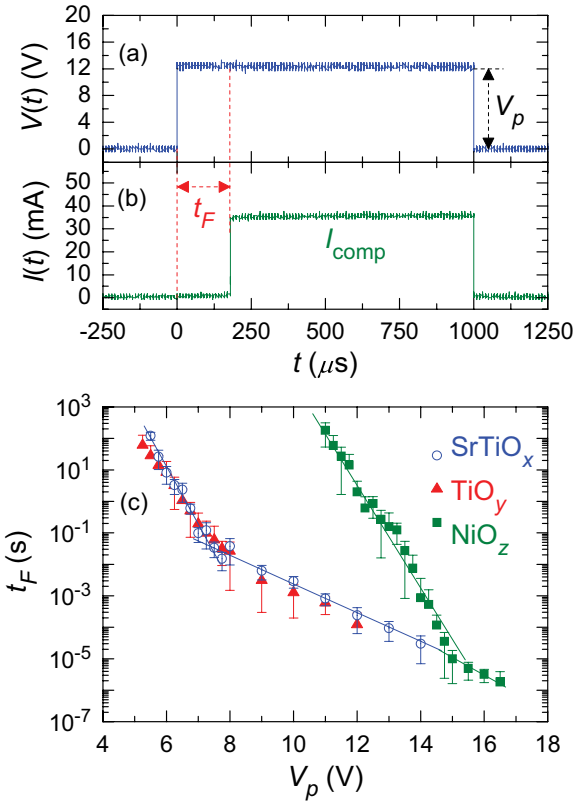

Figure 3. (*a*) Application of a pulse-waveform voltage signal with amplitude V_p and (*b*) resulting current $I(t)$. (*c*) V_p-dependence of forming times t_F for Pt/SrTiO$_x$/Pt [12], Pt/TiO$_y$/Pt and Pt/NiO$_z$/Pt cells.

sample through an avalanche process during the dielectric breakdown [7, 11, 12]. To avoid permanent damage to the cell, we applied the $I_{comp} \approx 30$ mA, through a 2N2369 switching transistor. Due to the I–V characteristics of the transistor, $I(t)$ increased slightly even when $V > V_F$.

We found that V_F increased significantly with an increase in ν for Pt/SrTiO$_x$/Pt, Pt/TiO$_y$/Pt and Pt/NiO$_z$/Pt cells. As represented by the open blue circles in figure 2(*c*), for the Pt/SrTiO$_x$/Pt cells, V_F increased from ~6 V to ~16 V when ν was increased from 20 mV s^{-1} to 2 MV s^{-1} [12]. The ν-dependence of V_F showed two different relationships, with a crossover at $\nu^{co} \approx 2000$ V s^{-1}. Notably, the values of V_F for $\nu > \nu^{co}$ increased faster than those for $\nu < \nu^{co}$. Pt/TiO$_y$/Pt and Pt/NiO$_z$/Pt cells also showed this behaviour, albeit with different ν^{co} values; they are also plotted in figure 2(*c*) using closed red triangles and closed green squares, respectively.

A pulse-waveform voltage signal of amplitude V_p was also used to drive the forming process, as shown in figures 3(*a*) and (*b*). A sudden increase in $I(t)$ occurred (figure 3(*b*)) when t reached the forming time t_F (figure 3(*a*)). In this measurement, we also applied $I_{comp} \approx 30$ mA, through a 2N2369 switching transistor. We investigated the V_p-dependence of t_F by gradually increasing V_p, and found that t_F decreased drastically with V_p for the Pt/SrTiO$_x$/Pt, Pt/TiO$_y$/Pt and Pt/NiO$_z$/Pt cells, as shown in figure 3(*c*). As indicated by the open blue circles, t_F for the Pt/SrTiO$_x$/Pt cells decreased from ~100 s to ~10 μs when V_p increased from 5.5 to 14 V [12]. The V_p-dependence

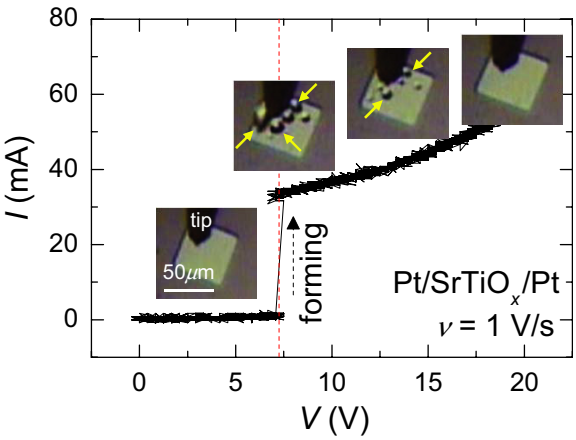

Figure 4. Bubble development on the top Pt electrode during the forming process with $\nu = 1$ V s^{-1}.

of t_F also exhibited two different relationships, with a crossover at $V_p^{co} \approx 7.5$ V. The t_F-values for $V_p < V_p^{co}$ decreased faster than those for $V_p > V_p^{co}$. The Pt/TiO$_y$/Pt and Pt/NiO$_z$/Pt cells also showed this behaviour with different V_p^{co}-values, as depicted by the closed red triangles and closed green squares, respectively.

We also observed bubbles developing on the top Pt electrode during the forming process with $\nu < \nu^{co}$ or $V_p < V_p^{co}$ for the Pt/SrTiO$_x$/Pt, Pt/TiO$_y$/Pt and Pt/NiO$_z$/Pt cells. Figure 4 shows the development of bubbles on the top Pt electrode during the forming process of a Pt/SrTiO$_x$/Pt cell. We applied

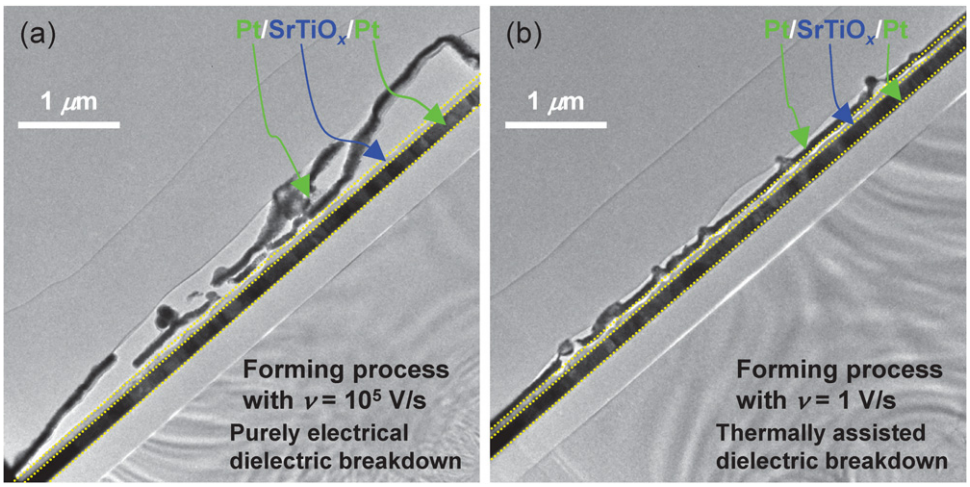

Figure 5. Cross-sectional TEM image of the top Pt electrode after the forming process with (*a*) $\nu = 10^5\,\mathrm{V\,s^{-1}}$ (purely electrical dielectric breakdown) and (*b*) $\nu = 1\mathrm{V\,s^{-1}}$ (thermally assisted dielectric breakdown).

a triangular-waveform voltage signal with $\nu = 1\,\mathrm{V\,s^{-1}}$ ($\nu < \nu^{co}$), and then took pictures by synchronizing a charge-coupled device camera, a synthesized function generator and a digital oscilloscope. The left picture shows a clean top Pt electrode at zero voltage. When we increased the voltage below the forming voltage, the top Pt electrode remained clean. When the current increased abruptly, i.e. during the forming process, a few bubbles developed locally, as indicated by the yellow arrows in the second picture. However, as shown in the third picture, when we increased the voltage above the forming voltage, the bubbles gradually disappeared. Further increases in the voltage resulted in the Pt electrode returning to the clean status shown in the right picture. Similar observations have been made for the bipolar resistance switching (BRS) forming process in Pt/TiO_2/Pt cells [10]. The BRS is the other type of RS phenomena, which required both voltage polarities to reversibly change the resistance values between low- and high-resistance states. Our observation indicates that bubbles can be formed during the URS forming process as well.

Recently, we proposed that the URS forming process in Pt/$SrTiO_x$/Pt cells occurs by two different mechanisms, depending on the ν-values or V_p-values: a purely electrical dielectric breakdown ($\nu > \nu^{co}$ or $V_p > V_p^{co}$) or a thermally assisted dielectric breakdown ($\nu < \nu^{co}$ or $V_p < V_p^{co}$) [12]. According to the literature [11], the former is due to electronic processes, such as single-electron collision ionization, space charge production from collision ionization or field emission from the electrodes. In the latter, the Joule heating of the pre-breakdown current plays a role, which is highly related to ion migration inside the sample. Free ions can be accelerated by the field and can thereby induce current flow inside the sample, finally leading to an avalanche breakdown of ions. As shown in figures 2 and 3, the forming processes in Pt/TiO_y/Pt and Pt/NiO_z/Pt cells show the same experimental behaviour as the URS forming process in Pt/$SrTiO_x$/Pt cells. This indicates that the forming processes follow the same physical mechanisms in Pt/$SrTiO_x$/Pt, Pt/TiO_y/Pt and Pt/NiO_z/Pt cells.

For $SrTiO_x$, TiO_y and NiO_z thin films, O^{2-} ions can act as free ions for the forming process in the thermally assisted dielectric breakdown. When we apply positive voltage to the top electrode, O^{2-} ions migrate to the top electrode. Underneath the top Pt electrode, O^{2-} ions can change into O_2 gas according to the oxygen exchange reaction [2, 3]:

$$O^{2-} \leftrightarrow \frac{1}{2}O_2(g) + V_O'' + 2e^-, \qquad (1)$$

where O^{2-} and V_O'' denote oxygen ions on regular lattice sites and oxygen vacancies, respectively. The O_2 gas can lift up the top Pt electrode and form bubbles on the top electrode, as shown in figure 4. Recently, Kwon *et al* [9] reported that the URS in Pt/TiO_2/Pt cells occurs due to the formation and disruption of the oxygen-deficient phase of TiO_2 (Ti_nO_{2n-1}: the Magnéli phase). This report is very consistent with our scenario; that is, the O_2 gas leaves oxygen vacancies inside the oxide materials according to equation (1), and these then form local conducting channels.

3.3. Origin of the fatal damage to the top electrodes during the forming process

We found that the fatal damage to the top Pt electrodes occurs during the forming process of the purely electrical dielectric breakdown ($\nu > \nu^{co}$ or $V_p > V_p^{co}$) in Pt/$SrTiO_x$/Pt, Pt/TiO_y/Pt and Pt/NiO_z/Pt cells. Figure 5(*a*) shows a cross-sectional TEM image of the Pt/$SrTiO_x$/Pt cell after the forming process with $\nu = 10^5\,\mathrm{V\,s^{-1}}$ ($\nu > \nu^{co}$). The top Pt electrode was drastically blown off after this forming process. Most top Pt electrodes were burned out and turned black in colour. Conversely, as shown by the cross-sectional TEM image of figure 5(*b*), after the forming process with $\nu = 1\,\mathrm{V\,s^{-1}}$ ($\nu < \nu^{co}$, a thermally assisted dielectric breakdown), the top Pt electrode was still attached to the $SrTiO_x$ thin film. As explained in figure 4, a few bumps can form on the top Pt electrode because of the O_2 bubbles, which can develop during the forming process.

For purely electrical dielectric breakdown during the forming process, the top Pt electrodes can be blown off due to a sudden current flow. The aforementioned microscopic models of this breakdown are quite complicated, and depend highly

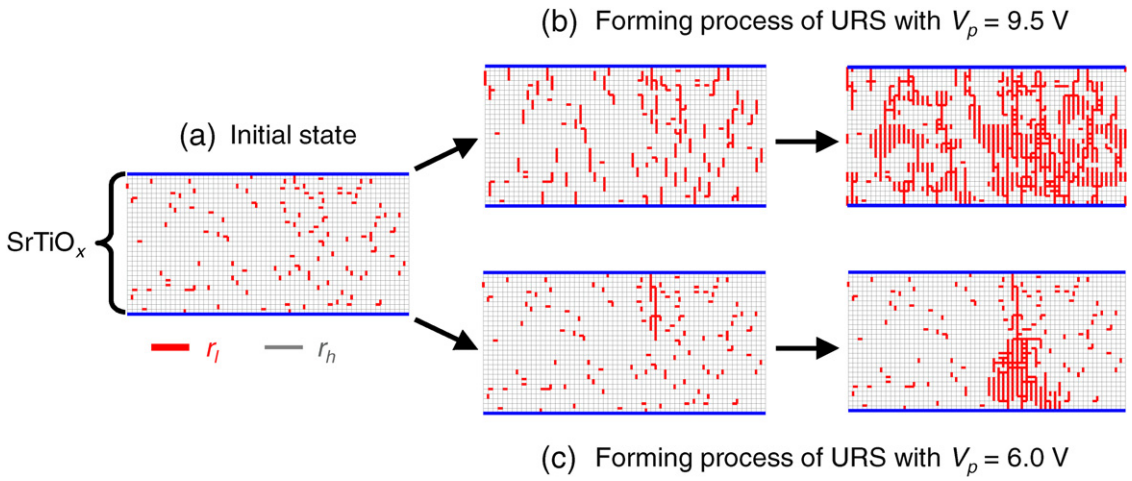

Figure 6. (*a*) Initial configuration of circuit breakers in the RCB network model. Procedural snapshots of the circuit breakers during the forming process with (*b*) $V_p = 9.5$ V and (*c*) $V_p = 6.0$ V.

on the material system [11]. However, the concept of sudden ionization is common for all microscopic models. The sudden ionization of many charges results in a sudden current flow, which shocks and burns the top Pt electrodes. Conversely, the pre-breakdown current can flow for the forming process of the thermally assisted dielectric breakdown. This current flow allows oxygen ions to move by Joule heating effects. Therefore, a few charges can flow, which shocks the top Pt electrodes to a lesser degree and hence does not blow them off.

To fully understand the fatal damage to the top Pt electrodes, we performed a computer simulation based on the random circuit breaker (RCB) network model. The RCB network model is a new kind of percolation model that can explain RS phenomena independently of materials systems [7]. Based on this model, we approximated the switching medium as a network composed of circuit breakers with bistable resistance states: low-resistance r_l (red circuit breakers) and high-resistance r_h (black circuit breakers), as shown in figure 6. We determined switching rules between r_l and r_h, which are governed by the voltage across each bond. Details of this percolation model and the computer simulation method are described elsewhere [7]. This percolation model has been very successful in explaining most experimental findings, including voltage-/current-driven RS [7], scaling behaviour [13–15], large $1/f$ noise [16], and coexistence of URS and BRS in a cell [17, 18]. One advantage of the RCB-network-based model computer simulations is that we can look at a snapshot of the circuit breaker configurations for each state of interest, and visualize what happens during each process.

Figure 6 presents procedural snapshots of the circuit breakers during the forming process. We found that many conducting channels are formed during the process with the higher V_p, see figure 6(*b*). Although we started from the same initial state as figure 6(*a*), fewer conducting channels were generated by decreasing the V_p value in the forming process, as shown in figure 6(*c*). For the forming process where $v > v^{co}$ or $V_p > V_p^{co}$, considerable current should flow due to the many conducting channels. The nanometre-thick top Pt electrodes might be blown off because they cannot withstand the large voltage stress and current flow. Recently, Yang *et al* [10] reported that the physical deformation of the top electrodes disappeared when the cell size was decreased to a nanometre. This experimental result is quite consistent with our scenario, as, after the forming process, smaller cell sizes tend to include fewer conducting channels.

As described above in section 1, the physical deformation of the top electrodes during the forming process is one crucial obstacle preventing the adoption of URS in computing circuits [9]. According to our observations, we could easily overcome this forming process problem by applying a voltage pulse $v < v^{co}$ or $V_p < V_p^{co}$. However, to achieve the forming process within the time scale of a few nanoseconds, we should apply a voltage pulse of $v > v^{co}$ or $V_p > V_p^{co}$. To prevent fatal damage to the top electrodes, they must be able to withstand large voltage stresses and current flows. We therefore deposited top Pt electrodes of 40, 60, 80, 100 and 120 nm thickness on the $SrTiO_x$ thin films. The top Pt electrodes were well preserved above 80 nm, even when we used a forming process with an applied voltage pulse $v > v^{co}$ or $V_p > V_p^{co}$. Thick electrodes might effectively endure large voltage stresses and current flows. Consequently, the overall robustness of the electrode might determine the minimum time required for the forming process.

3.4. Control of the number of conducting channels during the forming process

Many conducting channels in nanometre thin films cause inevitable problems to the realization of RRAM devices. It is widely accepted that the physical mechanism of the URS is the formation and rupture of nanoscale conducting channels [1–3, 7–9, 12–18]. Due to the chaotic nature of percolating behaviour in conducting channels [13–15], the URS for many conducting channels covers a wide variation in RRAM performance. Moreover, much of the current should flow through these many conducting channels and consume a large amount of power. Many researchers have thought that a smaller number of conducting channels would improve device properties such as retention, endurance and uniformity [19].

Therefore, to decrease the number of conducting channels, researchers have tried to optimize the fabrication of thin films, decrease the size of the electrodes or develop new measurement skills. However, because of the diverse experimental findings in this rapidly expanding field, there has been considerable confusion and controversy.

Through our percolation model, we can control the number of conducting channels through the forming process. The forming process is crucial to the URS because it generates conducting filaments and determines their percolating connectivity. We found that a forming process employing lower v and V_p made fewer conducting channels. Therefore, we expect that the device performance of RRAM can be enhanced by proper control of the forming process.

4. Conclusion

We have gained further understanding of the fatal damage to the top electrode when forming reversible resistance switching in material systems by investigating the physical mechanisms of the process. By employing a computer simulation based on a percolation model, we found that many of the conducting channels that formed were caused by a purely electrical dielectric breakdown. This forming process can destroy nanometre-thick top Pt electrodes, because they cannot withstand the large voltage stress and current flow.

Acknowledgments

This research was supported by grants from the National Research Foundation of Korea funded by the Korean Ministry of Education, Science, and Technology (Grant Nos 2009-0080567 and 2010-0020416, (MK) 2012-0005637 (BK) 2010-0015066, (BSK) 2011-0004004, and (SBL) NRF-2011-354-C00031).

References

[1] Ramanathan S 2010 *Thin Film Metal-Oxides: Fundamentals and Applications in Electronics and Energy* (New York: Springer)
[2] Waser R and Aono M 2007 *Nature Mater.* **6** 833
[3] Waser R, Dittmann R, Staikov G and Szot K 2009 *Adv. Mater.* **21** 2632
[4] Dearnaley G, Stoneham A M and Morgan D V 1970 *Rep. Prog. Phys.* **33** 1129
[5] Lee M-J *et al* 2007 *Adv. Mater.* **19** 73
[6] Lee M-J *et al* 2007 *Adv. Mater.* **19** 3919
[7] Chae S C *et al* 2008 *Adv. Mater.* **20** 1154
[8] Lee M-J *et al* 2009 *Nano Lett.* **9** 1476
[9] Kwon D-H *et al* 2010 *Nature Nanotechnol.* **5** 148
[10] Yang J J, Miao F, Pickett M D, Ohlberg D A A, Stewart D R, Lau C N and Williams R S 2009 *Nanotechnology* **20** 215201
[11] O'Dwyer J J 1973 *The Theory of Electrical Conduction and Breakdown in Solid Dielectrics* (Oxford: Clarendon Press)
[12] Lee S B, Yoo H K, Chang S H, Gao L G, Kang B S, Lee M-J, Kim C J and Noh T W 2011 *Appl. Phys. Lett.* **98** 053503
[13] Lee S B, Chae S C, Chang S H, Lee J S, Seo S, Kahng B and Noh T W 2008 *Appl. Phys. Lett.* **93** 212105
[14] Lee J S, Lee S B, Chang S H, Gao L G, Kang B S, Lee M-J, Kim C J, Noh T W and Kahng B 2010 *Phys. Rev. Lett.* **105** 205701
[15] Lee J S and Kahng B 2011 *Phys. Rev.* E **83** 052103
[16] Lee S B, Park S, Lee J S, Chae S C and Chang S H 2009 *Appl. Phys. Lett.* **95** 122112
[17] Lee S B, Lee J S, Chang S H, Yoo H K, Kang B S, Kahng B, Lee M-J, Kim C J and Noh T W 2011 *Appl. Phys. Lett.* **98** 033502
[18] Yoo H K *et al* 2011 *Appl. Phys. Lett.* **98** 183507
[19] Ahn S-E *et al* 2008 *Adv. Mater.* **20** 924